

Aircraft-produced Ice Particles (APIPs) in Supercooled Clouds and the Probable Mechanism for their Production

WILLIAM L. WOODLEY

Woodley Weather Consultants, Boulder, Colorado

THOMAS J. HENDERSON

Atmospherics, Inc., Fresno, California

BERNARD VONNEGUT

State University of New York at Albany, Albany, New York

GLENN GORDON

Department of Atmospheric Science, University of Wyoming, Laramie, Wyoming

ROBERT BREIDENTHAL

College of Engineering, Department of Aeronautics and Astronautics, University of Washington, Seattle, Washington

SHIRLEY M. HOLLE

Holle Computer Consultants, Boulder, Colorado

(Manuscript received 5 November 1990, in final form 17 March 1991)

ABSTRACT

This paper presents the results of studies of aircraft-produced ice particles (APIPs) in supercooled fog over Mono Lake, California. The King Air 200T cloud physics aircraft of the University of Wyoming and three other aircraft (a Piper Aztec, a Cessna 421-C, and a T-28) were involved in the tests. The King Air served as the monitoring aircraft when the other aircraft were tested and as both the test and monitoring aircraft when it was tested.

The studies demonstrated that the King Air produces APIPs. The ice crystals, in concentrations up to several hundred per liter, are initially quite small and of almost uniform size, and they grow to larger nearly uniform sizes with time. APIPs production is most likely at low ambient temperatures and high power settings, and when the gear and flaps are extended.

APIPs were not detected from the other aircraft. The Piper Aztec and Cessna 421 aircraft were tested on days on which an APIPs signature was produced by the King Air. The T-28 aircraft was tested when the fog-top temperature was greater than -6°C and neither the T-28 nor the King Air produced APIPs under these conditions.

Homogeneous nucleation appears to be responsible for the observed APIPs signature, although the exact mechanism for nucleation is not known. In addition, there is the suggestion that a weaker APIPs signature may be generated by heterogeneous nucleation, when the cooling in the prop-tip vortex falls short of that thought necessary for homogeneous nucleation (i.e., $\sim -39^{\circ}\text{C}$).

1. Introduction

From the inception of cloud microphysical studies, aircraft have been used to make internal cloud measurements. In most of these studies, little attention has been directed to the possibility that the aircraft might be affecting the parameters studied, even though this

possibility has been pointed out since 1948. For example, early Project Cirrus reports suggested that the vortices that form at the wing tips and particularly from the propeller tips might produce large numbers of ice crystals (Langmuir et al. 1948; Vonnegut 1948; General Electric 1952; Ludlam 1956; Havens et al. 1981) during an airplane's penetration of a supercooled cloud. This idea did not, however, receive much discussion in the open literature and at scientific conferences, nor were such effects the subject of much research.

Corresponding author address: Dr. William L. Woodley, 11 White Fir Court, Littleton, CO 80127.

In recent years, Rangno and Hobbs (1983, 1984) have directed renewed attention to a phenomenon that they call APIPs (aircraft-produced ice particles). Although not the first to discover this phenomenon, they are the first to systematically measure and document it using their B-23 research aircraft. These APIPs were noted at temperatures as warm as -8°C and in abnormally high concentrations ($>1000\text{ l}^{-1}$) and were generally rather uniform in size with modal diameters between 100 and 300 μm . They found that APIPs are contained in a relatively narrow cylindrical region of cloud, with the axis of the cylinder oriented initially along the aircraft flight track. The diameter of the cylinder increased with time, being 300 m after 5 min. In concentration (at the center of cylinder), size distribution, and appearance, Rangno and Hobbs noted that APIPs are similar to the ice crystals produced by dry-ice seeding. However, the latter forms a vertical curtain of crystals and affects a much larger volume of cloud.

When Rangno and Hobbs (1983) wrote their article, they left the mechanism for the formation of APIPs open to question. Although they noted that "cooling due to rapid expansion of the air in the region of the aircraft" might be a cause of APIPs, they focused initially on ice nucleation by the fuel exhaust products (i.e., lead combining with iodine vapor to form lead iodide) and on the production of ice particles associated with icing of the aircraft.

In their second paper, Rangno and Hobbs (1984) presented circumstantial evidence that APIPs were produced in the wake of a Hawker-Sidley 748, twin-engine, turbine, propeller-driven aircraft, powered by kerosene. Because kerosene contains no lead additives, they ruled out the exhaust products as a possible mechanism for the formation of APIPs.

By October 1985, Hobbs (1985) had come to the view "that the most likely mechanism for APIPs is the adiabatic expansion and cooling of air in the vortices produced at the tips of propeller blades and aircraft wings." Hobbs credited Vonnegut (1948) with first having suggested this mechanism and for having revived it. Lending support to the adiabatic expansion and cooling explanation for APIPs are the quantitative estimates by Vonnegut (1986) of the potential cooling produced in prop-tip vortices and the increase in nucleation rate that would result from such a decrease in temperature.

Working in the context of the 1984-1985 field program of the Sierra Cooperative Pilot Project (SCPP), Gordon and Marwitz (1986a) attempted to find APIPs in the wake of a turboprop Aerocommander 690-B operated by Aero Systems, Inc. The Aerocommander released SF_6 gas during its traverse of the cloud and this pass was followed by the University of Wyoming's King Air, which contained sophisticated navigational equipment and instrumentation to detect both the SF_6 and any generated ice particles. The SF_6 was detected by the King Air on one pass but no ice particles were

found, leading Gordon and Marwitz (1986a) to conclude that the Aerocommander aircraft did not produce APIPs. The authors also predicted that this might be a general result for turboprop aircraft because of their "substantially subsonic propeller tip speeds."

Gordon (1986) and Gordon and Rodi (1990) report on a continuation of the APIPs studies in 1986 as a part of the SCPP. This time the test and the measurement aircraft was the Super King Air T200 aircraft of the University of Wyoming. By this time, Vonnegut's hypothesis that adiabatic cooling in the prop-tip vortices was the likely cause of APIPs was receiving increased attention, and Gordon's experiments were designed with this in mind.

Growing cumulus clouds were penetrated by the King Air at about -10°C at normal (1700 rpm) and high (2000 rpm) engine speeds. The clouds were then reentered in a search for APIPs. Only 2 of the 37 cloud penetrations following the initial traverse of the clouds showed evidence of APIPs. APIPs were particularly evident in one cloud with ice-crystal concentrations of nearly 2000 and 100 l^{-1} observed by 1D-C and 2D-C measurement probes, respectively. APIPs may have been produced in many of the other clouds, but vertical air motions could have carried them away from the path of the aircraft. Gordon identified this as a serious problem in any study of APIPs and concluded the following:

"While no firm conclusion can be drawn about the mechanism producing the APIPs, it is suggestive from this data that cooling at the propeller tips might be responsible since a much higher ice crystal concentration was observed at the higher rpm (larger ΔT)."

The accumulated evidence over the past 40 years, especially the quantitative evidence in recent years, suggests that APIPs are a real phenomenon. The mechanism for their production, however, is still unknown. This is the focus of this paper.

2. The Mono Lake APIPs Study (MOLAS)

Because of the potential importance of APIPs to cloud physics studies that have or will make use of aircraft to study the internal structure of clouds, it is crucial that the APIPs controversy be resolved and the implications of its resolution be assessed. This paper takes a step in this direction by presenting the results of APIPs studies in supercooled fog over Mono Lake, California. It builds on previous studies and focuses on the production of APIPs and on specification of the physical mechanism that is responsible for their generation. This effort is given the acronym MOLAS (Mono Lake APIPs Study) to facilitate the presentation.

The MOLAS effort has four objectives:

- 1) Confirmation of the findings of Rangno and Hobbs (1983, 1984) that aircraft produce APIPs.
- 2) Investigation of the Vonnegut (1986) hypothesis

that adiabatic cooling at the prop tips is responsible for the production of APIPs.

3) Systematic investigation of the production of APIPs by other aircraft types that have been and/or are involved currently in cloud microphysical investigations.

4) Assessment of the implications of the MOLAS findings to past and current microphysical research.

At the outset, it was decided to keep the initial experimentation as simple as possible by limiting the studies to supercooled fog. The natural microphysical variability in fog is small relative to the expected APIPs signal. This is not the case in convective clouds. In addition, there is a higher probability of sampling the cloud volume that has been disturbed by passage of the test aircraft in fog than in convective clouds in which strong vertical air motions may carry the aircraft plume away from its flight level on subsequent cloud passes.

3. Design of the APIPs tests

a. Experimental setting

The experiments were conducted over Mono Lake, California. Because of its unique geographical setting

and the general winter climatology of the area, Mono Lake provides an excellent outdoor laboratory for observing APIPs. The location is shown in Fig. 1.

The lake elevation is 1968 m above sea level and has a surface area of approximately 250 km². It has no outlet and is completely surrounded by higher terrain rising to 3500 m above sea level nearby to the west. During winter weather when a high pressure system is well established over California, the surface air east of the Sierra range is cold and fog occurs over Mono Lake and Mono Valley to the east. A temperature inversion of a few degrees may persist for periods of 3–5 days, and the fog, which forms beneath the inversion, is stabilized by condensation rates from the lake surface, which are equal to the droplet evaporation/sublimation at the top of the fog layer. The top of the fog is normally 250–300 m above the lake and surrounding land surface. The vertical temperature profile from ground level to fog top varies depending on the general weather pattern surrounding the high pressure system. Typically, the ambient air temperature at fog top is in the range from -2° to -6°C, and at ground level is in the range from -6° to -10°C. In cold conditions, however, fog-top temperatures can be as low as -15°C. The maximum areal extent of the fog is indicated in Fig. 1. When

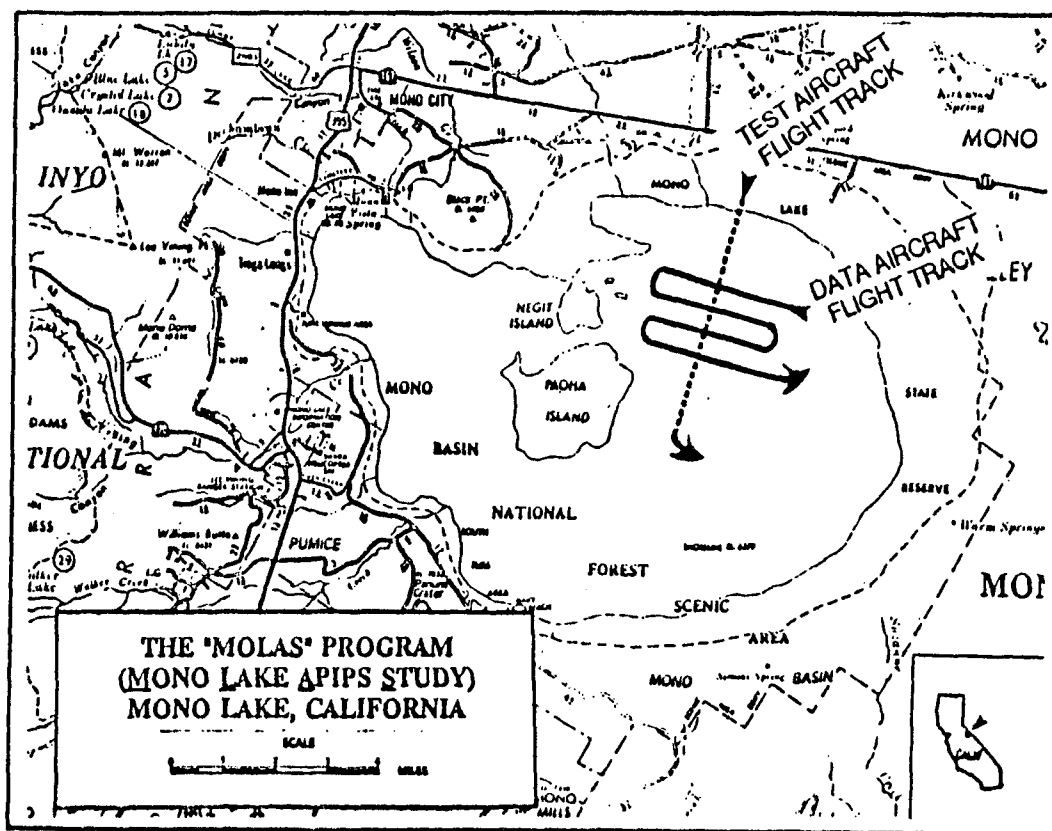


FIG. 1. Map showing the geographic context for the MOLAS (Mono Lake APIPs Study) program. The aircraft flight patterns have been superimposed.

present, the fog area is rarely less than the area of the lake.

b. Flight patterns

The APIPs studies involved flights of aircraft in the upper portion of a supercooled fog layer, followed by documentation of the physical changes in the fog after the passage of the aircraft. Primary documentation of internal fog structure is provided by the Particle Measuring Systems (PMS) probes on the King Air aircraft of the University of Wyoming.

The flight tests were simple in design and execution. A test aircraft made an initial test pass through the fog. The King Air 200T cloud physics aircraft followed closely behind the test aircraft until it entered the fog (Fig. 1). The scientist aboard the King Air set its pointer to the position where the test aircraft initially entered the fog and the pilot of the King Air then flew tracks that were orthogonal, or nearly so, to the track of the seeder aircraft (see Fig. 1). The test track was normally 3–4 km long, and the orthogonal flight legs of the cloud physics aircraft within the fog averaged approximately 2 km on either side of the track of the test aircraft. Each successive monitoring pass was made approximately 0.5 km down the track from the previous pass in order to avoid fog that had been disturbed previously by the monitoring aircraft.

When the King Air aircraft was both the test and monitoring aircraft, it made an initial test run into the fog, setting a navigational point 1 km before exiting from the fog. The King Air was then flown successively across the track in patterns that were nearly orthogonal to the initial track. In most cases, each successive monitoring pass was made approximately 0.5 km up the track from the previous pass.

In keeping with the hypothesis of Vonnegut (1986) that cooling at the prop tips is responsible for homogeneous nucleation of APIPs, the initial test of each aircraft involved a pass into the fog at maximum power setting. When the monitoring for this test was completed, subsequent tests were made in undisturbed fog at lower power settings. It was predicted that the high-power tests would be most likely to produce APIPs.

The key to these experiments was the air-relative navigation system aboard the King Air, which allowed the King Air to be flown back through previously sampled or disturbed air parcels. The method assumes a uniform horizontal and vertical wind field in the region of flight for the duration of the flight. This is a good assumption for Mono Lake fog. At a time or position chosen by the flight scientist, a reference point was established by initiation of the navigational algorithm. Integration of the air-relative displacement vector was started and the pilot then received a continually updated heading and distance back to the original point. The aircraft could then be piloted back to this point,

or a new point relative to the original reference could be set at a specified distance either up or down the track.

Since the MOLAS effort is designed to study APIPs, the monitoring aircraft was flown at relatively low-power settings to minimize any possibility that the aircraft might produce ice crystals, which might be ascribed erroneously to the initial test run. For all passes, the elapsed time between the time that the test aircraft first traversed a point and the time that the monitoring aircraft traversed it again was calculated. This was done to determine whether a relationship existed between the sizes of the ice crystals and the elapsed time since passage of the test aircraft.

c. Measurement systems

The hydrometeor concentrations, sizes, and habits were determined using two probes [manufactured by Particle Measuring Systems (PMS), Inc. of Boulder, Colorado] that are flown routinely aboard the University of Wyoming King Air 200T aircraft. The two probes are a forward scattering spectrometer probe (FSSP) and an OAP-2D-C (2D-C) probe. The 2D-P precipitation probe was not used in MOLAS because the fog hydrometeors remained fairly small. The FSSP detects particles from 2 to 30 μm in diameter in increments of 2 μm , and the 2D-C detects particles from 25 to 800 μm in intervals of 25 μm . A description of these probes, including 2D-C artifact rejection criteria, is given in Gordon and Marwitz (1986a). Water contents within the fog were estimated using Johnson-Williams instrumentation. Water contents were also estimated by integrating the output of the FSSP probe. More information on the University of Wyoming King Air data system can be obtained by referring to Endsley et al. (1986) and to Gordon and Marwitz (1986b).

4. Test results

a. Operational overview

During the winter 1989/1990 phase of the program, which began on 28 November 1989, there were 18 supercooled fog episodes: 3 in November 1989, 5 in December 1989, and 10 in January 1990. The daily weather log for this period can be found in Woodley et al. (1990). Several of these fog episodes were suitable for APIPs test flights. Over the course of six total flight days in December 1989 and January 1990, 28 experiments were conducted, including two experiments in which dry ice was dropped into the fog and two experiments that involved the use of the organic ice nucleant *Pseudomonas syringae*. After the initial test run, as few as 2 or as many as 6 monitoring passes were made at nearly right angles to the test track. The total number of monitoring passes was 114. Fog-top tem-

peratures were as warm as -5°C (on 4 December 1989) and as cold as -11°C (on 24 January 1990) on the flight days. A Piper Aztec, a Cessna 421C, and a T-28 were tested, in addition to the University of Wyoming King Air, for the production of AIPs. A summary of the results of all flight operations is provided in Tables A1 and A2 of the Appendix.

b. Natural fog conditions during flights in December 1989 and January 1990

The typical winter fog situation at Mono Lake involves a ridge of high pressure at the surface and aloft, and a cold moist layer near the surface that is capped by a strong inversion. After one or two days under these conditions, fog forms and fills much of the Mono Lake basin, as shown in Fig. 2 for 1 December 1989. Notice the fog that is banked against the Sierra Nevada Range to its west. The University of Wyoming King Air can be seen flying over the fog as its landing gear was being extended prior to fog entry. The reason for this flight configuration and the results it produced are discussed later in this paper.

Without exception, the fog on all days during MOLAS formed under stable conditions with cold moist air near the surface and drier, warmer air immediately above. A representative example is the fog on 2 December 1989. Its top was at 2060 m MSL at a temperature of approximately -8°C . The temperature rose to over $+8^{\circ}\text{C}$ only 500 m above the fog. A partial plot of temperature versus height is provided in Fig. 3.

A summary of the available pass measurements on 1 December 1989 is provided in Table A1, and for the rest of the MOLAS program in Table A2 of the Appendix. Note from Table A2 that the fog water contents typically averaged $0.20\text{--}0.25\text{ g m}^{-3}$. The mean (averages over 6 s) maximum droplet concentration was 90 cm^{-3} (standard deviation of 41 cm^{-3}) and the mean (6-s averages) droplet diameters ranged between $12\text{ and }19\text{ }\mu\text{m}$ for the test runs (the "0" pass numbers in the table). The natural ice-crystal concentrations from the 2D-C probe in the undisturbed fog near the time of the test runs averaged 8 crystals per liter (standard deviation of 5 crystals per liter), which is higher than was expected.

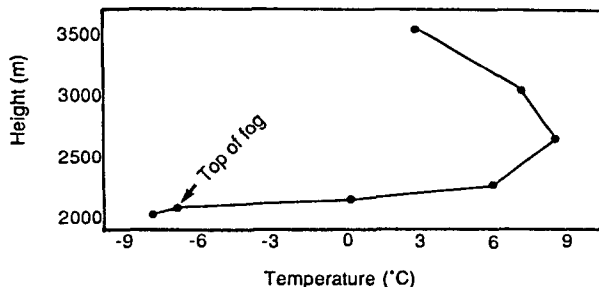


FIG. 3. Plot of temperature ($^{\circ}\text{C}$) vs height (m) over Mono Lake on 2 December 1989.

c. AIPs case studies

Two case studies are discussed in this subsection to demonstrate the reality of AIPs in Mono Lake su-



FIG. 2. Photographs from a Piper Aztec of the Mono Lake basin covered by supercooled fog on 1 December 1989. The view is to the west and shows the University of Wyoming King Air with gear down.

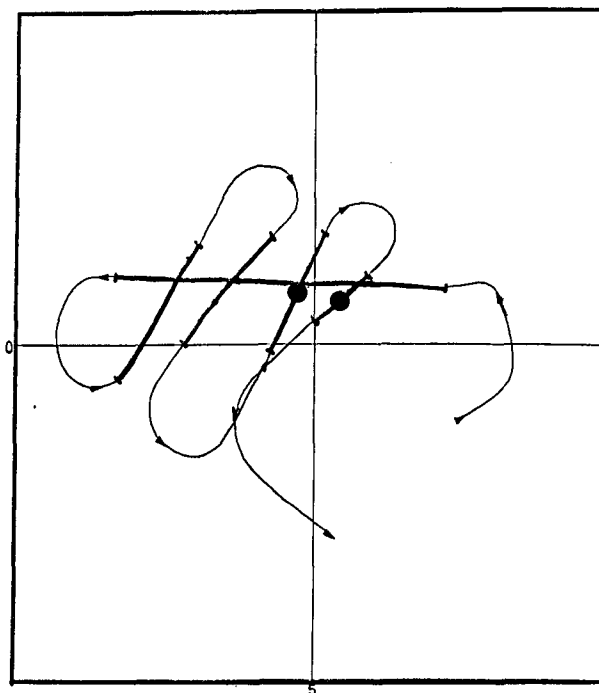


FIG. 4. Flight track of the University of Wyoming King Air on 2 December 1989. The heavy bold portions of the track indicate where the aircraft was in the fog. The dark circles indicate where an apparent AIPs signature was detected.

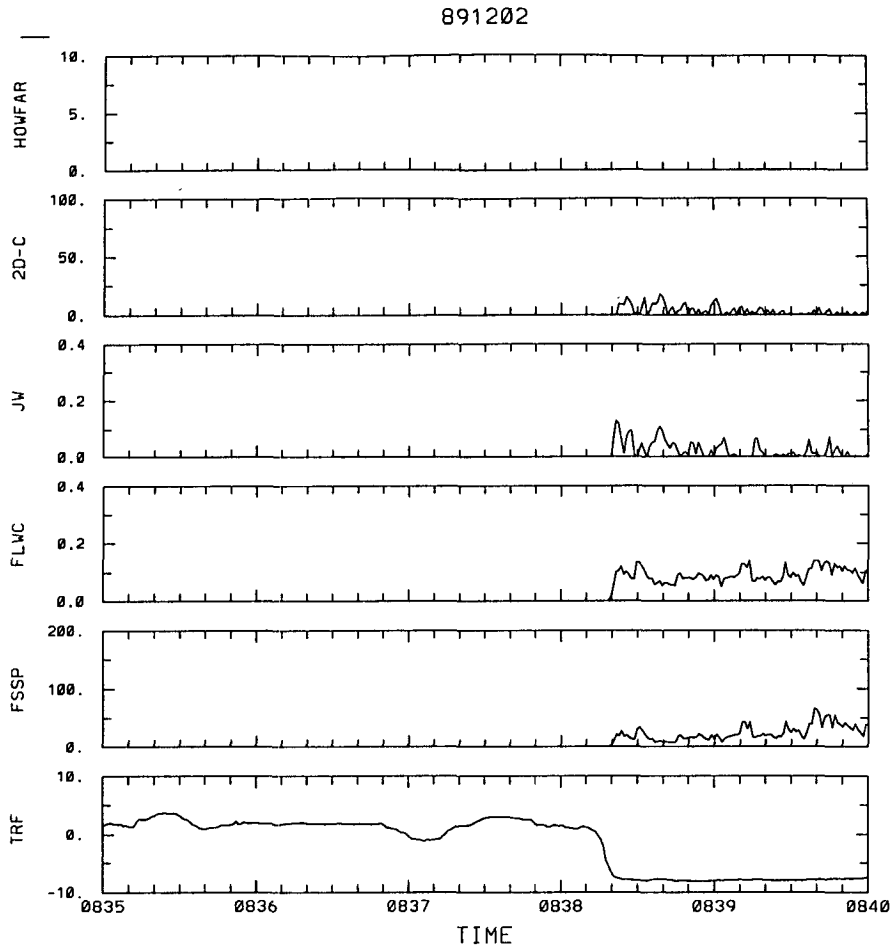


FIG. 5. Line plots of selected aircraft measurements. The top plot of the parameter HOWFAR gives the distance of the aircraft from the navigation point that was set along the test track. The vertical line in each HOWFAR plot represents the initial navigation point. When the distance from the point is "0," the aircraft has returned exactly to the setpoint. The scale on the ordinate is in kilometers, and in this and in all plots the scale on the abscissa is time in 10-s increments. The second plot is the ice-crystal concentrations (l^{-1}) as measured by the 2D-C probe. The third and fourth plots are the fog liquid water content ($g\ m^{-3}$) as measured by Johnson-William instrumentation and by integration of the output of the FSSP probe, respectively. The fifth plot is the droplet concentration (cm^{-3}) from the FSSP probe. The sixth and final plot is the ambient temperature ($^{\circ}C$) from the reverse-flow thermometer.

percooled fog. (All test cases are addressed by Woodley et al. 1990.) These cases are compared to seeding signatures produced by dry ice and by the organic nucleant *pseudomonas syringae*. The purpose of these seeding tests was to see whether a seeding signature could be detected and then to determine how it compared to the APIPs signature.

On 1, 2, and 3 December 1989, an obvious APIPs signature was produced by the King Air when it was flown at high power and maximum rpm settings with the landing gear and the flaps extended. No obvious signature was produced on these days when the gear and flaps were retracted. The possibility that weaker, secondary, APIPs signatures may have been produced

at lesser power settings and other flight configurations is discussed in a later section. No APIPs were detected during tests of the other aircraft even when they were flown at high power settings with their gear and flaps extended.

A representative example of an obvious APIPs signature when the King Air was flown at 1900 lb of torque and 1900 rpm with the gear and the flaps down was obtained on 2 December 1989. This test was an attempt to reproduce the APIPs signature of 1 December 1989, when the King Air was operated at a high-power setting with the landing gear and flaps down. Due to a tape recording malfunction, no data were recorded on this day and evidence for APIPs was ob-

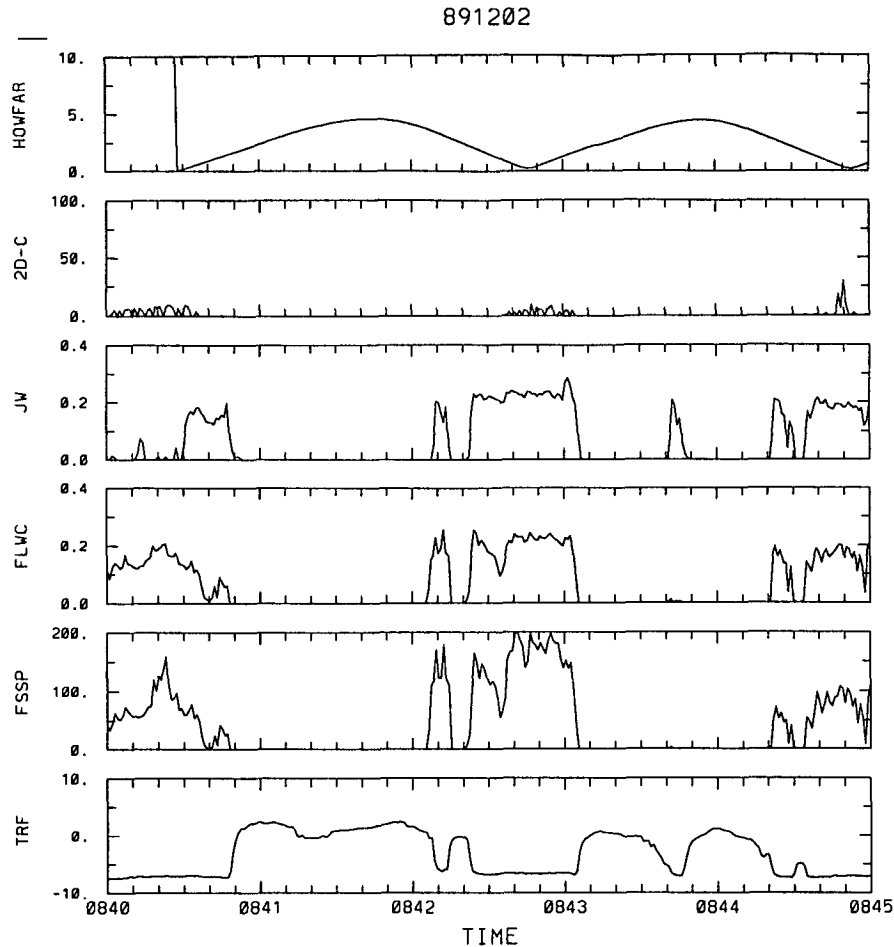


FIG. 5. (Continued)

tained from the real-time 2D-C plots aboard the aircraft.

Before presenting the results, it is important to first discuss the figures that will be used in the presentation. The flight track of the University of Wyoming King Air on 2 December 1989 during the first APIPs test is shown in Fig. 4. The dimensions of the plot are $10 \times 10 \text{ km}^2$. The heavy bold portion of the track indicates where the aircraft was in fog. The test pass is the long bold portion of the aircraft track in fog at the outset of the track. The dark circles indicate where an apparent APIPs signature was detected. Note that for this case, it was not until the third and fourth monitoring passes that this took place. The track of Fig. 4 and all subsequent flight tracks have been plotted relative to Pahoia Island, which is near the center of Mono Lake. The test track has not been moved with the wind in the plots.

Line plots of selected aircraft measurements for this case are provided in Fig. 5. Each figure has six plots.

The top plot of the parameter HOWFAR gives the distance of the aircraft from the navigation point that was set along the test track. The vertical line in each HOWFAR plot represents the initial navigation point. When the distance from the point is "0," the aircraft has returned exactly to the reference point. The scale on the ordinate is in kilometers, and in this and all plots the scale on the abscissa is time in 10-s increments. The second plot is the ice-crystal concentrations (l^{-1}) as measured by the 2D-C probe. The third and fourth plots are the fog liquid water contents (g m^{-3}) as measured by Johnson-William instrumentation and by integration of the output of the FSSP probe, respectively. The fifth plot is the droplet concentration (cm^{-3}) from the FSSP probe. The sixth and final plot is the ambient temperature ($^{\circ}\text{C}$) from the reverse-flow thermometer.

Upon examining the line plots of Fig. 5, two peaks in the 2D-C concentrations of nearly 100 crystals per liter are obvious during the third and fourth monitoring passes. Although they are decidedly higher and more

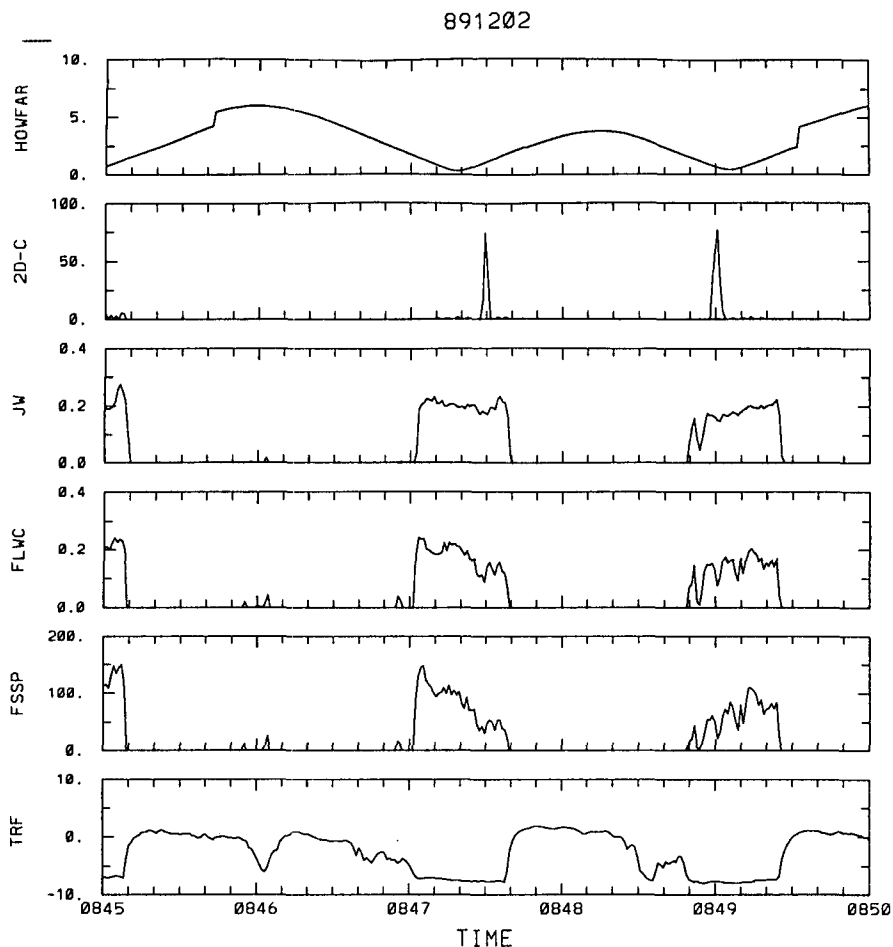


FIG. 5. (Continued)

peaked than the natural background evident during the test run from about 0838 to nearly 0841 LST, they are not proof of APIPs generation.

Figures 6 and 7 provide representative pictures of the 2D-C images during the test run and the four monitoring passes. The vertical lines in each panel are 800 μm long and the particles can be scaled by using this line as a reference. The times (s) in the left margin of each panel of Fig. 7 are the elapsed times between the passage of the test aircraft (the King Air in this case) and the times that the monitoring aircraft (the King Air) intercepted the seeding track.

The imaged particles in Fig. 6 were sampled during the test pass, which was the first fog penetration of the day. They all appear to be ice crystals of assorted sizes with a maximum concentration of 18 crystals per liter. A few of the particles appear to be columnar in form, which is the expected habit for a fog temperature of -8°C . How and why these ice crystals were produced in the undisturbed fog is unknown; it may be the result of a local source of ice nuclei in the Mono Lake area.

The imaged particles in all but the top panel of Fig. 7 were sampled during the monitoring passes. Nothing unusual is evident for the first monitoring pass of the King Air. It is not until the second, third, and fourth monitoring passes that a pattern begins to emerge. Notice how uniform in size the particles are within each panel and how they increase in size with time. This suggests a common origin for the particles, as might be the case if the test aircraft itself had generated the ice crystals.

This apparent APIPs signature should be compared with that discussed by Rangno and Hobbs (1983) from their studies of convective and layer clouds using their B-23 research aircraft. There is great similarity between the two apparent signatures even though the studies were done at different times, in different cloud types, and from different research aircraft.

Quantification of the picture evident in Fig. 7 is provided in Fig. 8 in which the mean, median, and modal ice-particle sizes are calculated from the 2D-C observations for each monitoring pass. The calculations are

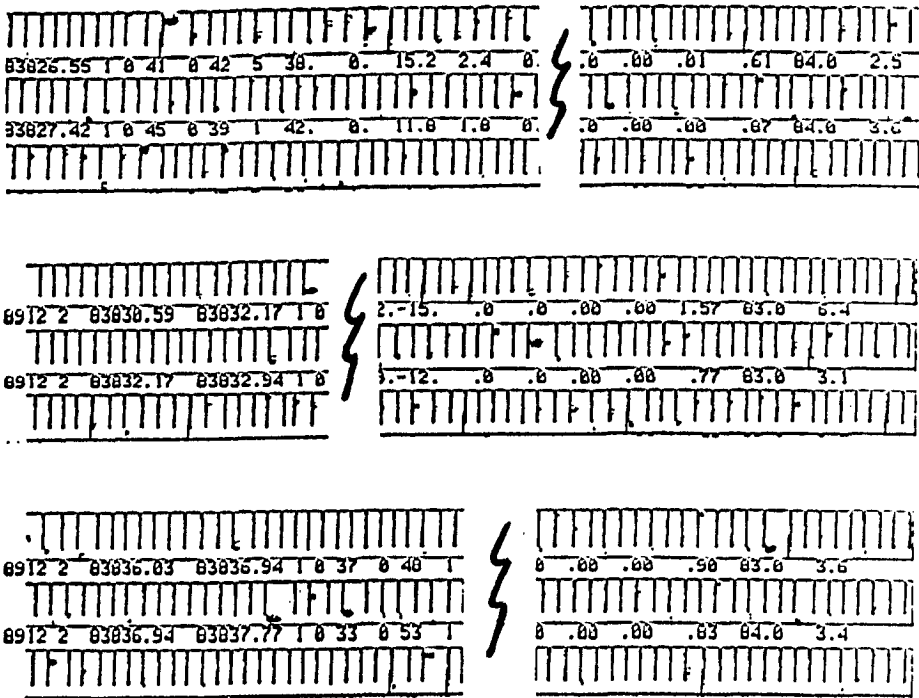


FIG. 6. A representative picture of the 2D-C images on 2 December 1989 during the test run. The vertical lines in each panel are $800 \mu\text{m}$ long and the particles can be scaled by using this line as a reference.

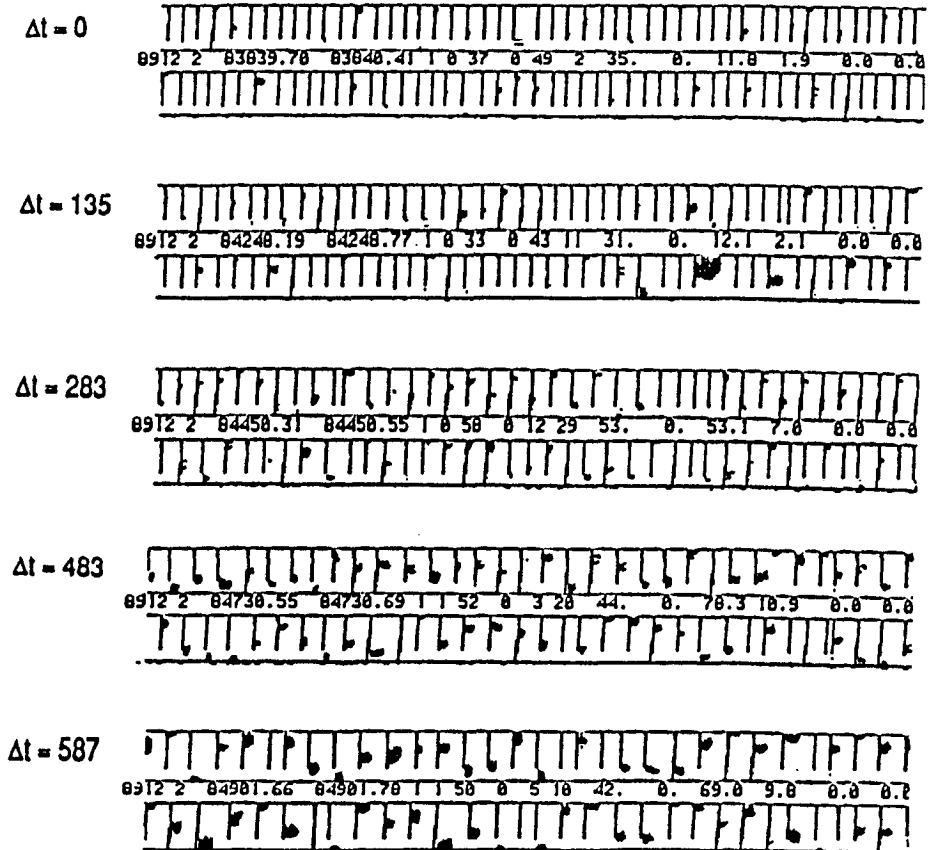


FIG. 7. A representative picture of the 2D-C images on 2 December 1989 during the test run and the four monitoring passes. The vertical lines in each panel are $800 \mu\text{m}$ long and the particles can be scaled by using this line as a reference. The times (s) at the left margin of each panel are the elapsed times between the passage of the test aircraft (the King Air in this case) and the times that the monitoring aircraft (the King Air) intercepted the test track.

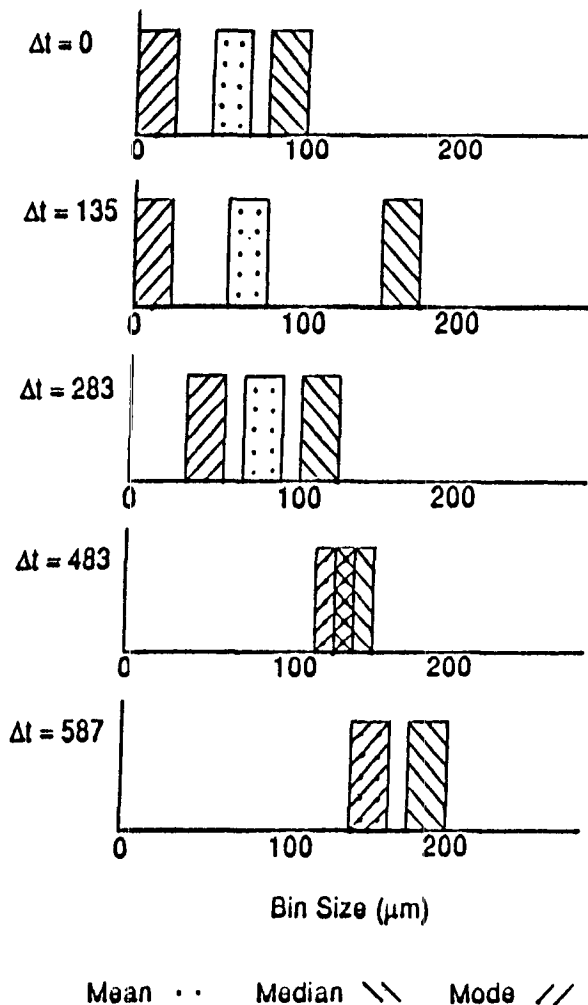


FIG. 8. Mean, median, and modal ice-particle sizes for each monitoring pass. The calculations are for the 5 s centered on the maximum detected ice-crystal concentration.

for the 5 s centered on the maximum detected ice-crystal concentration. Note the near uniformity in particle sizes, especially on the third and fourth monitoring passes. This behavior, coupled with the anomalous ice-crystal concentrations, is characteristic of the APIPs signature.

The last experiment of the day involved the release of 100 g of *Pseudomonas syringae* organic nucleant. The motivation for the tests was to see how the signature of a nucleant compared to the APIPs signature produced by an aircraft. Woodley and Henderson (1990) address this case extensively. Approximately 5 min after release of the nucleant, maximum ice-crystal concentrations of 155 crystals per liter were detected as the monitoring aircraft traversed the test track (see Table A2). These ice crystals were small initially, and they grew larger with time while maintaining their rel-

ative uniformity in size. This seeding signature is remarkably similar to the APIPs signature of Fig. 7.

APIPs testing ended on 4 December 1989 and resumed on 24 January 1990. The temperature near fog top on 24 January was -11°C . The first test of the day involved the King Air, which was flown with the gear and flaps up at 1900 lb torque and 2000 rpm. Prior to this day, the only obvious APIPs signatures had been produced by the King Air when its gear and flaps were extended.

The flight track and line plots for this case are shown in Figs. 9 and 10, respectively. The first, second, and third monitoring passes appear to have been made through an APIPs plume with crystal concentrations of nearly 250 l^{-1} on the second monitoring passes. The plume was not, however, intercepted on the fourth monitoring pass.

The 2D-C images (Fig. 11) support the interpretation that the first, second, and third monitoring passes intercepted the APIPs plume. The particles appear to be of uniform size and they are decidedly larger with each successive pass. Plots of the mean, median, and modal ice-crystal sizes quantify this impression (Fig. 12). The ice-crystal growth rate for this case is approximately $0.5\ \mu\text{m s}^{-1}$ at a temperature of -11°C and a water content of slightly less than $0.20\ \text{g m}^{-3}$.

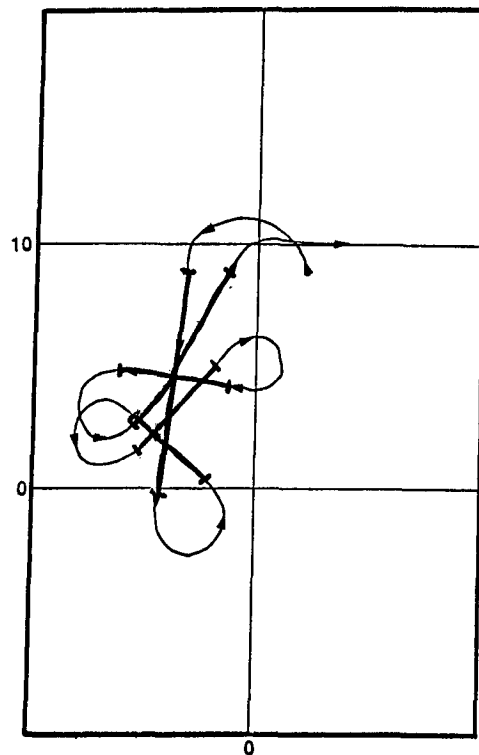


FIG. 9. The flight track for the test run beginning at 0849 PST 24 January 1990.

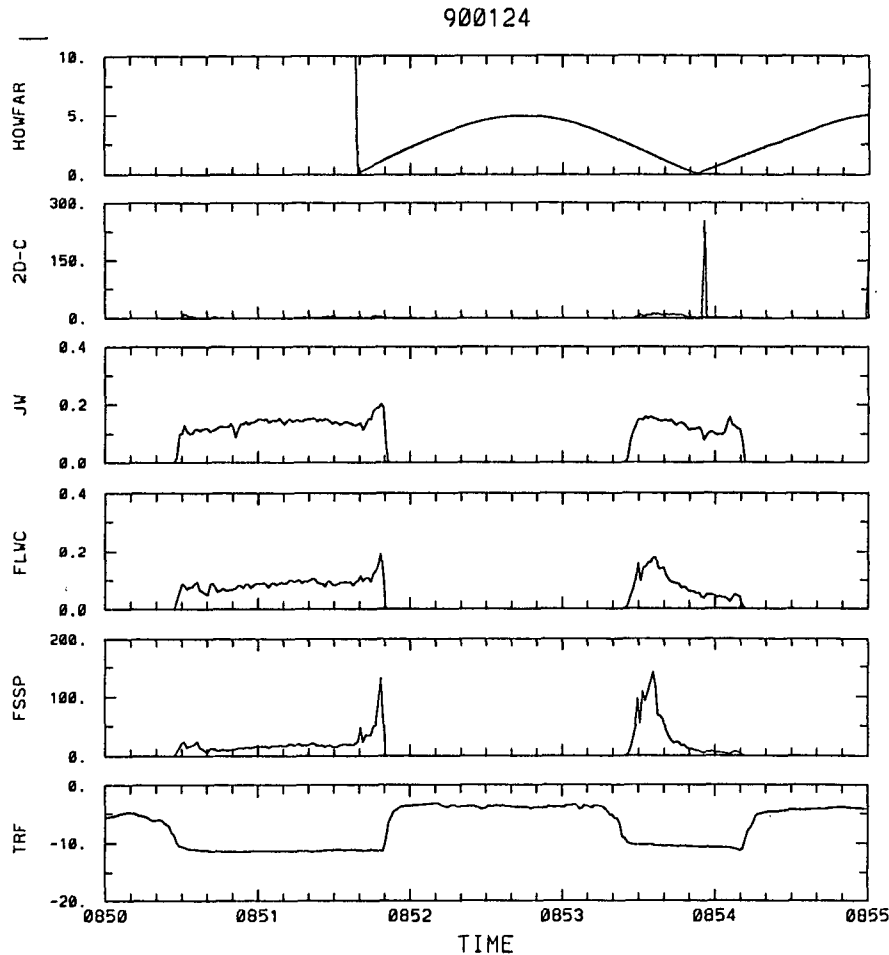


FIG. 10. The line plots of flight measurements for the test run beginning at 0849 PST 24 January 1990.

Our failure to detect the APIPs plume on the fourth monitoring pass of this case suggests that caution must be exercised in stating unequivocally that a particular test case did not produce APIPs. If the APIPs plume can be missed on one or two monitoring passes of an obvious APIPs signature, one must at least admit the possibility that the APIPs plume might have been missed on all of the monitoring passes of another test case. Only in examining the totality of the data might one be justified in reaching definitive conclusions.

The last case study to be discussed in this paper occurred on 25 January 1990 and involved the drop of about 6 lb of dry ice from a Piper Aztec followed by monitoring by the King Air. Complete documentation of this case is provided by Woodley et al. (1990). The ice crystals generated by the dry ice were detected on all six passes in concentrations ranging from approximately 100 to over 500 l^{-1} (Table A2). The ice crystals were quite small and grew only slowly with time. The slow growth rate was likely dictated by the large number

of ice particles and the low water content in the fog, averaging approximately 0.1 g m^{-3} .

The ice-crystal signature from the dry ice differed from the typical APIPs signature in several respects. First, it was easier to detect the effect of dry ice because of the greater vertical extent of its plume as compared to an APIPs signature. Second, the number of induced ice crystals was greater with the dry ice. Third, the growth rate of the ice crystals in the dry-ice cases was slower than the ice crystals generated by the aircraft.

d. Ensemble results

In order to present the results of MOLAS in ensemble form, it was first necessary to find a simple way of quantifying the strength of the APIPs signature. For the purposes of this report, the APIPs signatures were stratified into the following levels or orders.

First-order APIPs signature: ice-crystal concentrations are at least three times the natural (2D-C) back-

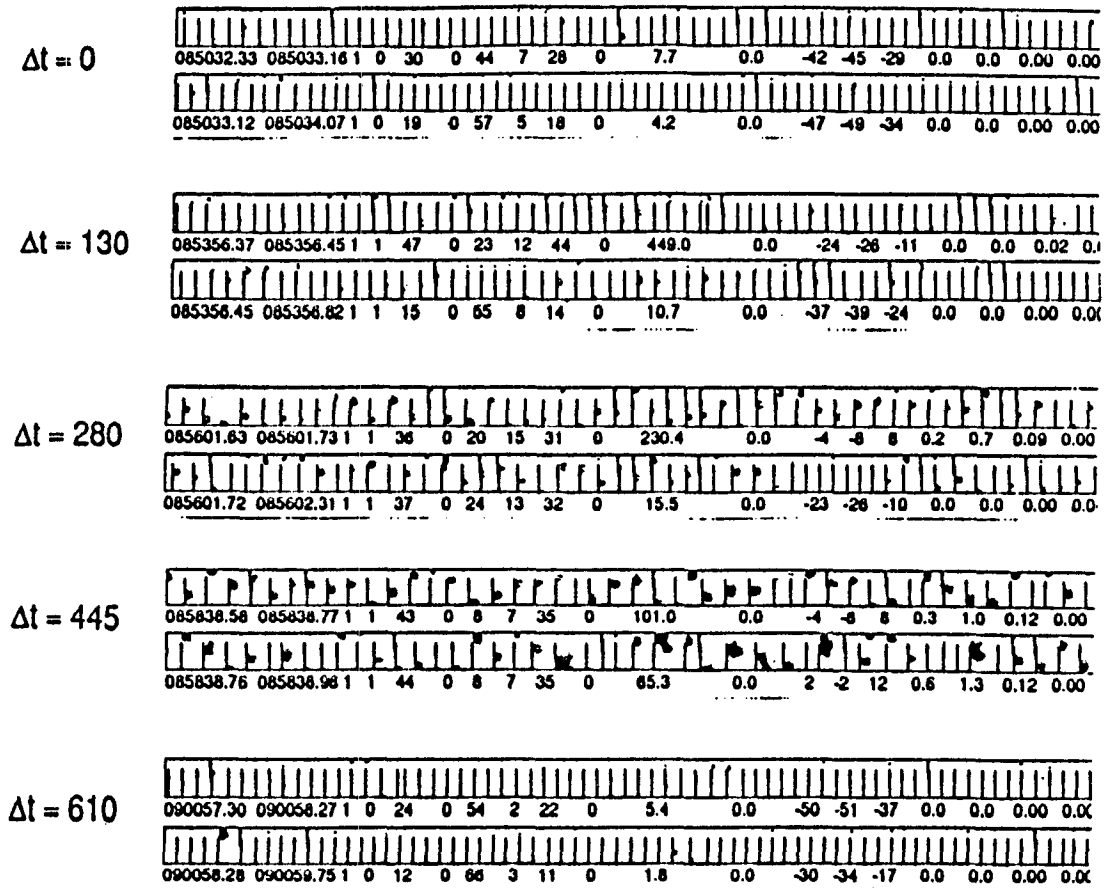


FIG. 11. The 2D-C images for the test run beginning at 0849 PST 24 January 1990.

ground on at least two of the monitoring passes.

Second-order APIPs signature: ice-crystal concentrations are at least three times the natural (2D-C) background on at least one of the monitoring passes.

Zero-order APIPs signature: ice-crystal concentrations are indistinguishable from the natural background and there is no evidence for an APIPs signature.

This simplistic approach takes into account the finding that even in strong APIPs cases the aircraft may miss the plume on one or more passes. Because most cases involved four or more monitoring passes, a first-order signature requires that only about 50% of the passes have ice-crystal concentrations at least three times the natural background, where the natural background is determined during the test run. A second-order signature requires that only about 25% of the passes have ice-crystal concentrations at least three times the natural background.

Classification errors are possible because it is uncertain whether the aircraft actually traversed the plume of the test aircraft. It is possible, therefore, that a second-order signature was, in fact, a first-order signature or

that a zero-order signature (i.e., no evidence of APIPs) was, in fact, a second- or even a first-order signature. Nevertheless, it was felt that in treating the data on an ensemble basis a clear picture would emerge.

The ensemble treatment of the data as a function of temperature and aircraft power setting and flight configuration is presented in Fig. 13. On the ordinate is temperature ($^{\circ}\text{C}$) and on the abscissa is aircraft power and flight configuration. Only data for the King Air are plotted, since none of the other aircraft tested produced APIPs at temperatures between -5°C and -11°C . Within a particular flight configuration (e.g., gear and flaps down), the aircraft torque and propeller rpm decrease from left to right. The two major flight configurations are gear and flaps up, and gear and flaps down. The two cases with intermediate configurations (i.e., gear up and flaps down, and vice versa) are plotted at the center of the abscissa. The plotted numbers (i.e., 1, 2, or 0) refer to the order of the APIPs signature with 0 indicating no detectable signature.

Examination of Fig. 13 reveals a fairly clear picture despite the uncertainties. The greater tendency for APIPs production, when the aircraft is flown with the

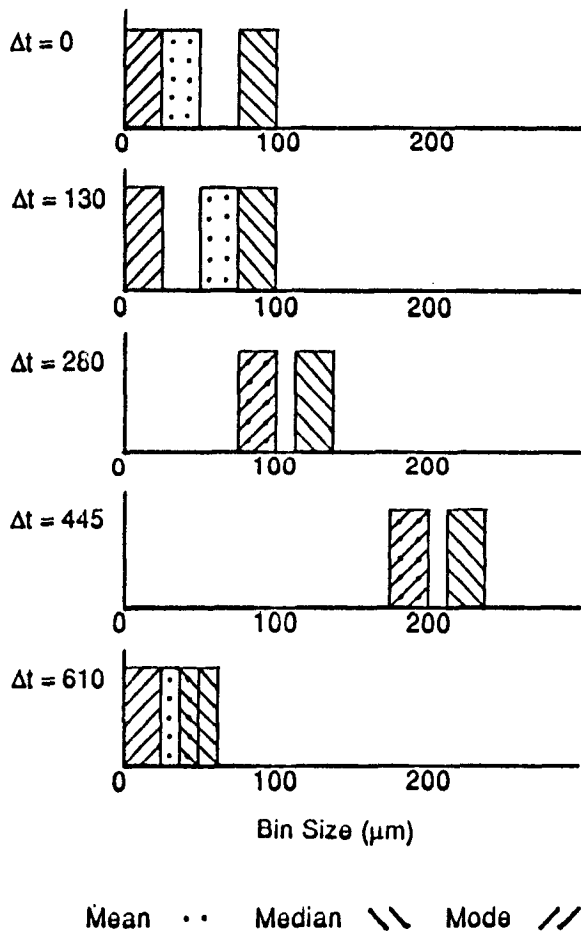


FIG. 12. The mean, median, and modal ice-crystal calculations for the test case beginning at 0849 PST 24 January 1990.

gear and flaps extended, is obvious in the plot. Note that 9 of the 19 plotted King Air cases showed evidence of an APIPs signature.

The first-order APIPs signatures provided a unique opportunity to calculate the rate of growth of the ice crystals in a natural supercooled fog. The mean, median, and modal ice-particle sizes for those monitoring passes showing an APIPs signature were plotted versus time, and the plots, along with the least-squares best-fit lines, are shown in Fig. 14. The growth rates are rather small, ranging from 0.23, to 0.27, to $0.35 \mu\text{s}^{-1}$, depending on whether one uses the mean, modal, or median particle sizes, respectively, as the representative measure. This is at least a factor of two less than that found by Rangno and Hobbs (1983) in their APIPs studies.

In addition to the six first-order and three second-order APIPs cases plotted in Fig. 13, four of the ten zero-order cases showed signs of APIPs (see Woodley et al. 1990). In all four suspect cases (two on 3 December 1989 and two on 24 January 1990) the ice-

crystal concentrations were small, but the sizes of the few ice crystals and their 2D-C presentations made them appear to be APIPs. For each suspect pass, the mean, median, and mode particle sizes were checked using the best fits of Fig. 14, and in each case, the particle sizes fell within the envelope of the plotted points for the first-order cases. This suggests that APIPs may have been generated in these four cases even though they were identified as non-APIPs cases.

5. The physical mechanism for APIPs in supercooled clouds

The physical mechanisms commonly offered to explain the APIPs phenomenon are the nucleation of ice crystals by the aircraft engine exhaust, shedding of ice from the aircraft, and nucleation of ice crystals at the prop tips (see Rangno and Hobbs 1983). Although our choice for a mechanism is obvious from the preceding sections of this paper, it is important, nevertheless, to address all possible mechanisms for APIPs production and their physical basis.

For aircraft burning leaded fuel, there is a distinct possibility that the exhaust products will contain leaded compounds that will serve as ice nuclei. In aircraft burning kerosene such as the University of Wyoming King Air, however, no such products are produced. But the King Air has produced the APIPs signatures that have been documented in this paper. Therefore, it is not likely that aircraft exhaust is a factor in the production of these signatures. Rangno and Hobbs (1984) have also abandoned leaded exhaust as a cause of APIPs.

The shedding of ice splinters from an aircraft appears to be a candidate for the generation of APIPs until it is realized that on three of the six flight days in MOLAS a strong APIPs signature was produced on the initial run of the King Air into the fog. The aircraft was carrying no ice at this time and the rather low fog water content resulted in only a slow buildup of ice on the aircraft. In addition, if the shedding of ice from the aircraft is the explanation for APIPs, ice crystals should have been produced whenever there was an ice buildup on the aircraft. This was definitely not the case in MOLAS. There were numerous instances when the aircraft was carrying a load of ice and no APIPs were detected. Further, none of the other aircraft tested produced APIPs, and they carried some ice on their test runs. The evidence simply does not support ice splintering for the APIPs that were observed in the MOLAS effort. This may not, however, preclude the shedding of ice from the aircraft as a cause of APIPs under other circumstances.

The experimental evidence of MOLAS suggests that aerodynamic cooling at the prop tip is responsible for the generation of the APIPs that were produced by the King Air. The apparent relationship between the power

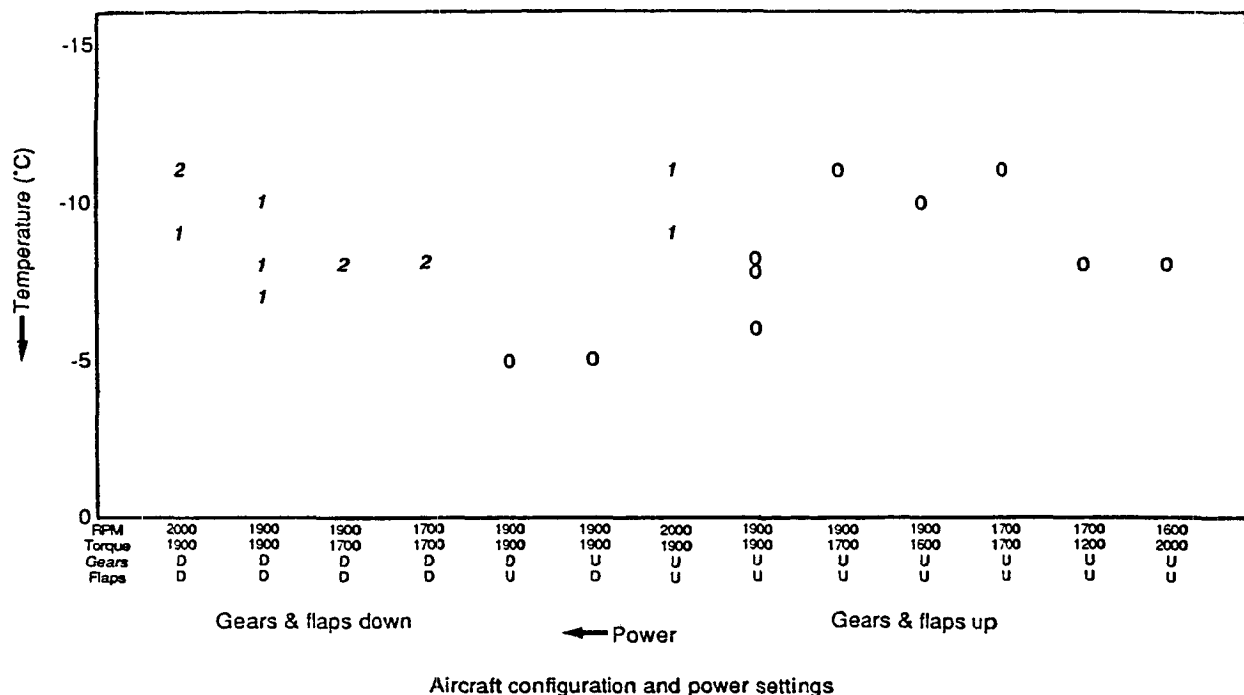


FIG. 13. Summary of the King Air APIPs tests. The order of the APIPs signature (first, second, or zero order) is plotted versus fog temperature and aircraft configuration and power setting.

setting of the aircraft engines and the production of APIPs supports this argument. It appears that at a given ambient temperature, the higher the power setting the more likely it is that APIPs will be generated. This agrees with the predictions of Vonnegut (1986).

Evidence for cooling at the prop tips of an aircraft is presented in Fig. 15, in which a condensation helix can be seen clearly coming off the prop of a four-engine aircraft. The air in this helix was cooled below the dewpoint at the time that it came off the propeller. At temperatures well below 0°C , one can readily envision this helix containing ice crystals that were generated at the prop tips.

Although it appears that how an aircraft produces APIPs has been explained, several questions remain unanswered. These include why the APIPs signature is stronger when the aircraft is flown in a "dirty" (i.e., gear and flaps down) configuration, and how the ice crystals are nucleated.

With the use of simple qualitative arguments based on aerodynamic theory, the first question might be answered. Consider a propeller-driven aircraft on which both the wings and the propeller blades are generating lift. Since the span of both the wing and each blade are finite, there must be a tip circulation associated with each lifting element. At a particular power setting the propeller blades are exerting forces on the air moving by its tips. If the power setting is maintained constant

and the gear and flaps are lowered, the drag on the aircraft increases and its airspeed decreases. Although the force exerted by the propeller may remain constant in this configuration, the impulse (force \times time) that the blade applies to the moving air parcel increases, which thereby increases the intensity of the circulation at the prop tips. This will further lower the pressure and the temperature in the prop-tip circulation. Under the right conditions, this cooling might be manifested as an APIPs signature.

Answering the question as to the mechanism of nucleation can be done by using the observations of MOLAS, the photograph in Fig. 15, and some order of magnitude arguments. The first step is the estimation of the total ice-crystal production along a 1-km track in a "typical" APIPs case. The MOLAS data suggest that after approximately 5 min the aircraft takes approximately 2 s or approximately 200 m to traverse the APIPs plume, giving a plume radius of 100 m. The plume cross-sectional area is approximately $3 \times 10^4 \text{ m}^2$, and the plume volume for the 1-km track is $3 \times 10^7 \text{ m}^3$. Based on the observations of MOLAS, the ice-crystal concentration in the APIPs plume is on the order of 100 l^{-1} , giving 3×10^{12} crystals within the 1-km plume.

The second step is the estimation of the volume in which the ice crystals were generated during the passage of the test aircraft in the fog. The photograph in Fig.

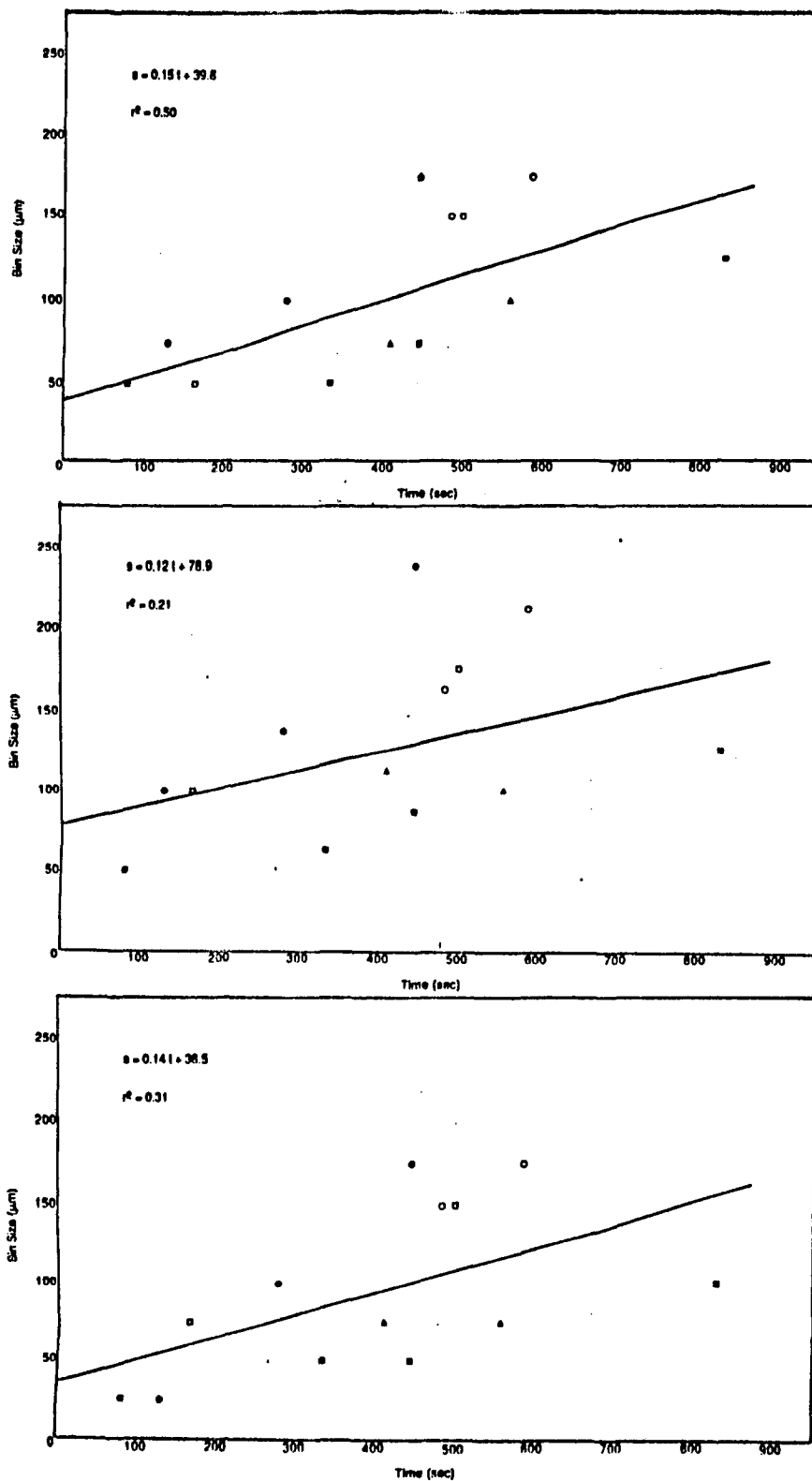


FIG. 14. Plot of mean, median, and modal 2D-C ice-crystal sizes versus time for the passes in first-order cases that showed an APIPs signature. The best-fit regression is shown by the solid line.



FIG. 15. A photograph from *Spacious Skies* of a condensation helix coming off the prop of a four-engine aircraft.

15 is helpful in this regard. Note that the thickness of the condensation helix is approximately 10% of the length of the aircraft propeller. Assuming that the same percentage applies to the King Air and its propeller blades of 1.25-m radius, this gives a thickness of approximately 12 cm for the cooled helix coming off its propeller. For ease of calculation, assume that the cross-sectional area on the prop in which the crystals are being produced is on the order of 100 cm^2 . For an aircraft traveling at 100 m s^{-1} and its propellers rotating at 1800 rpm, the air is flowing past the propeller at approximately 250 m s^{-1} . In 10 s, the aircraft traverses 1000 m while 2500 m of air pass the propellers. Therefore, the volume in which APIPs are produced is $2.5 \times 10^7 \text{ cm}^3$ for each propeller blade.

The third step is the estimation of the initial ice-crystal concentration off each propeller blade. The ice-crystal total of 3×10^{12} within the plume 5 min after the test run is a good approximation of the total number of crystals produced by the aircraft. When distributed within the volume of $2.5 \times 10^7 \text{ cm}^3$, the concentration is $1.2 \times 10^5 \text{ cm}^{-3}$. Because there are a total of 6 propeller blades on the twin-engine King air, this gives an initial APIPs concentration of $0.2 \times 10^5 \text{ cm}^{-3}$ per blade.

Having made an order of magnitude estimate of the initial concentration of APIPs, the question arises as to what mechanism of nucleation produced these ice crystals. Heterogeneous nucleation is a candidate, but the calculated initial ice-crystal concentration far exceeds the probable concentration of natural ice nuclei in the free atmosphere (Mason 1957). Direct freezing of the fog droplets, which have a concentration of 100 cm^{-3} , is another possible mechanism for the generation of the initial ice crystals, but the measured droplet concentration is a factor of 200 less than the estimated initial ice-crystal concentration.

The most likely explanation for the APIPs is some type of homogeneous process. Only such a process can produce ice crystals in such high concentrations. The laboratory research of Vonnegut (1948), Schaefer

(1954), and Maybank and Mason (1959) on the production of ice crystals by adiabatic expansion of moist air supports this point of view. For example, Maybank and Mason produced between 10^6 and 10^7 cm^{-3} from the expansion to -40°C of clean moist air. Considering the uncertainties, this agrees well with our estimates above. If the air was clean and devoid of ice nuclei, no ice crystals were produced by expansion to warmer final temperatures. When Maybank and Mason added artificial ice nuclei to the ambient moist laboratory air, ice crystals were produced at warmer final temperatures.

Despite these strong indications, the exact method of nucleation in MOLAS is unknown. It should be the focus of field and laboratory tests.

6. Discussion

Based on all of the evidence, one must conclude that APIPs is a real phenomenon that is produced by nucleation at the prop tips. The mechanism of nucleation is not known with certainty, although some type of homogeneous process is the most likely candidate. Which aircraft produce APIPs and under what conditions must still be determined.

A remaining important question is whether APIPs signatures are produced at and below a threshold temperature or whether they are produced over a broad range of temperatures. Although it cannot be proven at this juncture, we suspect that some APIPs are produced by heterogeneous nucleation over a range of temperatures and that the APIPs signature is enhanced once the temperature zone for homogeneous nucleation has been reached.

This is a matter of utmost importance. If APIPs are produced solely by homogeneous nucleation, it will be a relatively simple matter to avoid the conditions under which a particular aircraft produces APIPs, once those conditions have been specified. If APIPs are produced by both homogeneous and heterogeneous nucleation at the prop tips, however, the conditions for their production may be impossible to avoid. It is crucial, therefore, to investigate this possibility in future tests.

At this point in our research it is important to proceed cautiously with respect to past cloud microphysical research. Not enough is known about the production of APIPs as a function of aircraft type, configuration, and power setting to warrant a critique of past studies. The studies that are potentially the most affected are those in which repeated aircraft cloud penetrations were made at high power settings and/or low temperatures to infer the evolution of cloud properties, especially the conversion of water to ice. In such studies, it is possible that the observations made on the second and third measurement passes might have been contaminated by an APIPs signature. The studies least affected would be those in which only a single measurement pass was made to infer the properties of an ensemble

of clouds. An APIPs signature obviously would not contaminate these observations because they were not made in the wake of the aircraft.

7. Summary and conclusions

The MOLAS effort indicates that the King Air produces APIPs whose production is a function of ambient temperature, the power setting of the aircraft (i.e., torque and rpm), and its configuration (i.e., clean or with gear and flaps down). The lower the ambient temperature and the higher the power setting, the more likely it is that the aircraft will produce APIPs. In addition, at a given temperature, the aircraft is more likely to produce APIPs if the gear and flaps are extended.

The APIPs ice crystals are readily detectable on the PMS 2D-C probe as the aircraft traverses the flight track of the test run. The particles in concentrations greater than 100 l^{-1} are initially quite small and of almost uniform size, and they grow to larger nearly uniform sizes with time. The APIPs signature is similar to that described by Rangno and Hobbs (1983) and similar also to that produced by our tests of the organic nucleant *Pseudomonas syringae*. It is different, however, from that produced by the tests of dry ice in which more but smaller ice particles were noted.

The mechanism for APIPs production appears to be cooling at the prop tips. At a given ambient temperature, APIPs were produced once a critical aircraft power setting was exceeded. Below that threshold no obvious APIPs signature was produced.

The shedding of ice from the aircraft is not a likely mechanism for the APIPs produced in the MOLAS effort. The icing of the aircraft and the supercooled liquid water contents did not show much variability from one test day to the other, and yet the strong APIPs signatures were produced only at high power settings (i.e., 1900 lb of torque and 2000 rpm). In addition, on three of the six flight days, the King Air's first run into the fog produced strong APIPs signatures. Since the aircraft was carrying no ice on the initial run, the shed-

ding of ice from the aircraft is not an explanation of the APIPs signature in these cases. This does not necessarily preclude an ice-shedding process for the production of APIPs in other cloud types and under heavy icing conditions.

The APIPs are likely produced by homogeneous nucleation because the natural concentration of ice nuclei cannot explain the probable initial ice-crystal concentrations exceeding 10^7 l^{-1} . It is possible, however, that some natural aerosol particles might be capable of causing nucleation in an extremely short time interval at the low temperatures produced by adiabatic cooling. This might account for an apparent secondary APIPs signature.

None of the other aircraft tested (Piper Aztec, Cessna 421-C, and a T-28) produced APIPs even when they were flown at high power settings with their gear and flaps down. The Piper Aztec and Cessna 421 aircraft were tested on days on which an APIPs signature was produced by the King Air. The T-28 aircraft was tested when the fog-top temperature was greater than -6°C and neither the T-28 nor the King Air produced APIPs under these conditions.

Based on the findings of MOLAS to date, it is possible that APIPs have been produced in past cloud microphysical studies in which repeated penetrations and monitoring of subject clouds by an aircraft were made. Clearly, additional APIPs testing in the context of MOLAS of the aircraft types used in these studies is imperative. Only with the results of these tests will a valid assessment of the impact of APIPs on the results and conclusions of these studies be possible.

Acknowledgments. This research was supported by the National Science Foundation under Grant AMT-8813846.

APPENDIX A

Data Summaries

TABLE A1. Pass data summary for MOLAS on 1 December 1989 when the data did not go onto the tape. The limited information was obtained from real-time plots aboard the aircraft.

Date	Begin time (PST)	Aircraft	Aircraft configuration	Power setting (rpm/torque or M.P.)	Total number of passes	TRF ($^\circ\text{C}$)	Comments
1 December	0855:00	K	C	1900/1600	1	-10	
1 December		K			2	-10	no evidence of APIPs signature
1 December		K	F and G	1900/1900	1	-10	
1 December		K			4	-10	obvious APIPs signature
1 December	0925:00	Aztec		2500/22 in.	1	-10	
1 December		K			3	-10	no evidence of APIPs signature
1 December		Aztec		2500/25 in.	1	-10	
1 December		K			4	-10	no evidence of APIPs signature

K = King Air, C = "clean" (i.e., flaps and gear up), F and G = flaps and gear down, M.P. = manifold pressure in inches of mercury, TRF = temperature from a reverse-flow thermometer

TABLE A2. Pass data summary for MOLAS exclusive of 1 December 1989.

Date	Begin time (PST)	Aircraft	Aircraft configuration	Power setting (rpm/torque or M.P.)	Avg TAS (m s ⁻¹)	Pass number	Δt (s)	TRF (°C)	Avg JWLWC (gm m ⁻³)*	FSSP				2D-C		Comments
										Concentration	\bar{d}		Max concentration (No. l ⁻¹)	\bar{d} (5-s mean size)		
										Min (6-s avg)	Max (6-s avg)	Min (μm)	Max (μm)	Min (1-s value)	Max (1-s value)	
2 December	0838:18	K	F and G	1900/1900	76	0	—	-7.8	0.25	10	128	11	20	18	54	2D-C con $\sim 10^{-1}$ throughout pass
2 December	0842:12	K	C		94	1	135	-6.5	0.30	22	173	11	12	9	72	no evidence of APIs signature
2 December	0844:24	K	C		92	2	283	-7.0	0.25	17	126	11	14	30	78	small APIs signature
2 December	0847:06	K	C		96	3	483	-8.0	0.25	4	108	12	14	74	136	definite APIs signature
2 December	0848:54	K	C		95	4	587	-8.2	0.20	3	98	11	15	76	166	definite APIs signature
2 December	0853:36	K	C	1700/1200	95	0	—	-8.0	0.25	9	124	10	21	9	51	normal setting for cloud penetration
2 December	0857:42	K	C		97	1	135	-7.5	0.25	6	144	10	12	0	116	
2 December	0859:24	K	C		102	2	270	-6.7	0.30	53	166	11	13	2	136	
2 December	0902:18	K	C		105	3	458	-8.0	0.30	6	151	12	14	1	49	
2 December	0904:36	K	C		100	4	539	-7.7	0.30	26	107	12	14	1	52	
2 December	0911:00	K	C	1900/1900	107	0	—	-8.2	0.15	4	18	19	22	15	45	
2 December	0913:30	K	C		98	1	131	-8.2	0.18	2	13	15	21	9	54	
2 December	0915:26	K	C		99	2	249	-8.0	0.08	9	18	18	21	13	54	JW reading may be in error; images suggest APIs
2 December	0917:48	K	C		95	3	438	-8.0	0.20	1	12	17	22	18	64	images suggest APIs
2 December	0920:06	K	C		92	4	570	-7.8	0.15	2	13	14	23	15	65	images suggest APIs, missed test track
2 December	0932:10	Cessna	F and G	1850/31 in.	—	0	—	—	—	—	—	—	—	—	—	test of Cessna 421 with gear and flaps down
2 December	0933:18	K	C		94	1	120	-8.0	0.18	2	22	15	22	7	48	
2 December	0935:30	K	C		90	2	217	-7.9	0.20	3	62	12	17	1	56	
2 December	0938:00	K	C		93	3	391	-8.4	0.20	1	89	11	17	2	38	
2 December	0940:30	K	C		94	4	480	-7.4	0.20	3	170	11	13	2	75	
2 December	0949:42	K	C		107	0	—	-7.7	0.17	8	75	11	16	5	52	drop of 6 lb of dry ice from Cessna 421
2 December	0952:30	K	C		96	1	190	-8.0	0.20	6	62	11	14	64	38	obvious glaciation signature
2 December	0955:12	K	C		105	2	318	-7.6	0.25	6	47	13	16	329	64	obvious glaciation signature
2 December	1008:33	Cessna	C		—	0	—	—	—	—	—	—	—	—	—	drop of 10 g of pseudomonas syringae from Cessna 421
2 December	1009:48	K	C		96	1	117	-8.0	0.25	10	102	11	13	1	54	no evidence of plume
2 December	1011:42	K	C		95	2	206	-7.6	0.20	9	135	11	14	1	59	no evidence of plume
2 December	1014:36	K	C		96	3	368	-7.8	0.20	27	126	11	12	2	65	no evidence of plume
2 December	1017:00	K	C		100	4	488	-7.5	0.20	2	104	10	17	2	107	no evidence of plume
2 December	1024:50	Cessna	C		—	0	—	—	—	—	—	—	—	—	—	drop of 100 g of pseudomonas syringae
2 December	1025:54	K	C		87	1	100	-7.7	0.20	62	109	10	11	2	148	no evidence of plume
2 December	1027:48	K	C		85	2	180	-7.6	0.20	19	146	11	12	1	60	no evidence of plume
2 December	1030:12	K	C		93	3	347	-7.6	0.20	2	87	10	17	155	85	obvious penetration of plume
2 December	1032:48	K	C		96	4	510	-7.2	0.20	18	125	10	12	9	134	still in plume
2 December	1036:06	K	C		97	5	692	-7.5	0.25	7	140	10	15	40	166	still in plume
3 December	0853:24	K	C	1900/1900	108	0	—	-6.8	0.20	5	67	12	18	3	50	
3 December	0856:24	K	C		99	1	125	-5.9	0.25	24	66	12	14	0	63	200- μm columns, low concentration, missed track
3 December	0858:06	K	C		97	2	260	-6.0	0.25	3	48	12	18	0	50	200-300 μm columns, possible weak APIs signature, missed track
3 December	0900:12	K	C		96	3	376	-6.3	0.20	11	65	12	16	1	54	
3 December	0902:12	K	C		93	4	500	-6.5	0.18	7	21	13	16	3	139	

3 December 0908:00	K	F and G	1900/1900	76	0	—	-7.7	0.25	3	63	13	20	8	41	high concentration of particles < 100 μm apparent AIPs signature
3 December 0912:12	K	C		97	1	165	-7.0	0.25	18	81	12	14	58	46	
3 December 0914:06	K	C		96	2	293	-7.3	0.25	4	68	12	16	23	88	most ice particles 100-200 μm most ice particles 200-300 μm
3 December 0916:18	K	C		93	3	500	-7.5	0.22	10	26	14	20	133	132	
3 December 0920:30	K	F and G	1900/1700	72	0	—	-8.0	0.30	4	16	14	21	13	44	possible weak signature, many particles ~ 100 μm in size many particles up to 300 μm in size a few particles up to 400 μm in size, probably missed most of AIPs plume a few large ice particles (500 μm)
3 December 0925:06	K	C		98	1	150	-8.0	0.20	20	54	12	15	2	40	
3 December 0926:42	K	C		93	2	285	-7.8	0.15	12	54	13	16	4	75	
3 December 0928:54	K	C		96	3	467	-8.0	0.20	4	63	12	15	60	120	a few particles of 300-400 μm
3 December 0931:12	K	C		96	4	580	-8.0	0.20	3	21	11	18	8	43	
3 December 0935:42	K	F and G	1700/1700	70	0	—	-8.0	0.20	2	19	14	23	10	45	many small particles 100-200 μm in diameter, may have missed track
3 December 0940:18	K	C		102	1	160	-7.5	0.20	5	18	15	19	53	69	
3 December 0942:12	K	C		100	2	312	-7.7	0.20	1	20	16	19	1	117	ice particles 200-300 μm in size, possible AIPs signature particles 300-400 μm in diameter just gear, no flaps
3 December 0944:00	K	C		95	3	485	-8.2	0.15	1	22	13	16	8	115	
3 December 0946:30	K	C		99	4	615	-7.9	0.20	8	21	14	15	2	34	only pass with slight suggestion of AIPs
3 December 0950:48	K	C	1600/2000	105	0	—	-8.0	0.18	12	30	13	15	6	54	
3 December 0953:48	K	C		95	1	155	-8.1	0.15	8	15	13	18	1	54	just flaps and no gear, check to see if pass was contaminated, considerable ice
3 December 0955:36	K	C		88	2	292	-7.8	0.20	2	31	12	18	9	62	
3 December 0957:48	K	C		93	3	396	-7.9	0.20	11	24	12	13	4	60	run of T-28 made at 2200 rpm and 30 in. on manifold pressure
3 December 0959:30	K	C		96	4	505	-8.0	0.20	5	24	12	14	10	60	
3 December 1001:24	K	C		95	5	660	-8.2	0.15	1	17	10	14	2	62	T-28 with gear and flaps down and at high power
4 December 0851:06	K	C	1900/1900	94	0	—	-5.0	0.20	2	63	12	21	6	117	
4 December 0854:54	K	C		95	1	133	-4.8	0.15	8	55	13	13	2	115	repeat of previous test
4 December 0857:06	K	C		95	2	283	-5.0	0.20	16	61	12	15	5	45	
4 December 0859:18	K	C		97	3	471	-5.0	0.15	7	55	12	16	7	54	run of T-28 made at 2200 rpm and 30 in. on manifold pressure
4 December 0901:36	K	C		94	4	568	-4.8	0.15	3	69	12	16	12	62	
4 December 0910:00	K	F	1900/1900	83	0	—	-5.2	—	2	101	11	17	12	60	T-28 with gear and flaps down and at high power
4 December 0914:30	K	C		94	1	135	-5.2	0.20	1	35	13	18	1	48	
4 December 0916:30	K	C		96	2	279	-5.2	0.25	1	33	14	16	3	87	repeat of previous test
4 December 0919:00	K	C		96	3	461	-5.5	0.20	8	92	12	18	5	43	
4 December 0921:06	K	C		98	4	602	-5.3	0.25	10	72	12	15	5	51	run of T-28 made at 2200 rpm and 30 in. on manifold pressure
4 December 0935:20	T-28	C	2200/30 in.	107	0	—	—	—	—	—	—	—	—	—	
4 December 0936:36	K	C		91	1	106	-6.2	—	4	33	13	15	14	45	T-28 with gear and flaps down and at high power
4 December 0938:54	K	C		102	2	176	-6.2	0.25	2	46	12	17	6	47	
4 December 0940:24	K	C		93	3	247	-6.1	0.20	15	55	12	17	10	55	repeat of previous test
4 December 0942:24	K	C		90	4	436	-5.8	—	8	39	12	17	8	41	
4 December 0948:40	T-28	F and G	2400/30 in.	—	0	—	—	—	—	—	—	—	—	—	repeat of previous test
4 December 0950:36	K	C		90	1	145	-5.7	0.20	9	24	12	16	14	62	
4 December 0952:42	K	C		98	2	232	-5.8	0.20	6	45	12	15	11	53	repeat of previous test
4 December 0954:36	K	C		94	3	321	-6.2	0.20	2	36	13	16	5	44	
4 December 0955:48	K	C		89	4	514	-6.1	0.20	4	57	11	14	11	52	repeat of previous test
4 December 1002:40	T-28	F and G	2400/30 in.	—	0	—	—	—	—	—	—	—	—	—	
4 December 1004:30	K	C		100	1	116	-5.7	0.20	3	29	12	14	7	62	repeat of previous test
4 December 1005:48	K	C		92	2	184	-5.8	0.18	6	47	12	15	8	42	
4 December 1007:30	K	C		88	3	307	-6.0	0.18	2	54	11	19	11	53	repeat of previous test
4 December 1009:42	K	C		95	4	414	-6.0	0.20	5	49	12	16	7	55	

TABLE A2. (Continued)

Date	Begin time (PST)	Aircraft configuration	Power setting (rpm/torque or M.P.)	Avg TAS (m s ⁻¹)	Pass number	Δt (s)	TRF (°C)	Avg Max JW LWC (gm m ⁻³)*	FSSP Concentration			2D-C		Comments	
									Min (No. cm ⁻³) (6-s avg)	Max (No. cm ⁻³) (6-s avg)	Δd (μm)	Max concentration (No. l ⁻¹) (1-s value)	Δd (5-s mean size)		
24 January	0850:30	K	2000/1900	109	0	—	-11.4	0.14	11	49	14	20	10	48	aircraft is clean
24 January	0853:30	K		92	1	130	-10.6	0.13	5	105	11	21	287	55	spike
24 January	0855:42	K		91	2	280	-11.0	0.11	8	16	15	20	145	99	smaller spike
24 January	0858:06	K		87	3	445	-10.8	0.12	4	22	14	24	71	166	spike
24 January	0900:30	K		86	4	610	-10.8	0.10	5	8	19	21	6	44	missed spike
24 January	0906:00	K	1700/1700	99	0	—	-11.3	0.12	12	50	12	18	4	57	aircraft is clean
24 January	0909:36	K		89	1	159	-10.5	0.10	6	48	11	20	4	65	nothing
24 January	0912:06	K		95	2	294	-10.7	0.11	9	33	11	17	17	85	weak possible spike
24 January	0914:42	K		90	3	534	-11.0	0.11	10	23	13	18	2	38	nothing
24 January	0916:48	K		93	4	630	-10.9	0.14	13	66	12	15	4	48	nothing
24 January	0922:54	K		100	0	—	-11.4	0.11	7	50	12	19	3	43	aircraft is clean
24 January	0925:54	K		88	1	130	-11.2	0.06	1	14	0	22	1	101	nothing, near fog top
24 January	0930:24	K		83	2	240	-11.5	0.08	12	34	12	18	1	146	nothing, thin fog
24 January	0932:18	K		82	4	590	-11.3	0.06	5	40	11	21	7	52	nothing
24 January	0947:30	K	2000/1900	78	0	—	-10.0	0.02	4	72	8	21	8	53	nothing
24 January	0951:18	K	F and G	92	1	125	-9.3	0.09	13	67	8	13	4	63	gear and flaps down
24 January	0953:06	K		91	2	254	-9.6	0.02	9	33	9	12	3	55	nothing, possibly too low
24 January	0955:06	K		86	3	420	-9.6	0.10	30	73	9	11	38	116	nothing
24 January	0957:12	K		86	4	564	-9.6	0.10	8	58	10	19	5	41	spike
24 January	0959:18	K		94	5	714	-9.5	0.04	28	93	10	11	10	62	nothing
25 January	0822:30	K	2000/1900	98	0	—	-9.4	0.07	11	123	10	17	3	35	not much, surprised not to detect a more definite signal with this configuration
25 January	0826:24	K		89	1	126	-9.4	0.08	11	58	9	12	2	26	clean aircraft
25 January	0828:42	K		85	2	309	-9.4	0.09	16	105	9	13	3	38	nothing
25 January	0831:12	K		89	3	411	-9.2	0.09	3	102	9	13	22	69	nothing
25 January	0833:00	K		88	4	558	-9.3	0.07	15	52	10	14	15	78	nothing
25 January	0835:36	K		89	5	704	-9.2	0.10	39	106	9	10	5	30	weak spike, all runs this far near same point
25 January	0837:36	K		90	6	840	-9.0	0.08	45	89	9	10	7	30	nothing, made up track
25 January	0846:30	K	2000/1900	79	0	—	-9.2	0.01	5	146	9	21	4	38	nothing
25 January	0850:24	K		90	1	80	-9.2	0.08	4	70	9	20	45	29	gear and flaps
25 January	0852:36	K		85	2	334	-8.9	0.11	9	115	9	17	22	44	spike
25 January	0855:06	K		91	3	445	-9.0	0.09	5	52	10	18	126	44	nothing
25 January	0857:18	K		83	4	596	-8.9	0.06	5	101	8	20	5	64	nothing
25 January	0900:06	K		96	5	831	-9.0	0.06	4	140	8	18	54	104	spike, 30 ft below initial track
25 January	0917:00	Aztec		—	0	—	—	—	—	—	—	—	—	—	nothing
25 January	0920:18	K		83	1	300	-8.8	0.02	1	95	0	13	—	—	drop of dry ice
25 January	0923:30	K		93	2	435	-8.9	0.08	4	27	10	12	298	33	spike, big within plume
25 January	0925:24	K		91	3	555	-8.8	0.05	4	47	9	13	241	34	spike
25 January	0928:18	K		87	4	723	-8.9	0.04	3	29	9	14	428	39	spike
25 January	0930:36	K		86	5	870	-8.7	0.03	4	38	7	18	400	51	spike, all passes across same point
25 January	0933:18	K		86	6	1050	-9.0	0.00	3	10	9	14	282	45	spike

* estimated from plots
 K = King Air, C = "clean" (i.e., flaps and gear up), F and G = flaps and gear down, M.P. = manifold pressure in inches of mercury, TRF = temperature from a reverse-flow thermometer

REFERENCES

- Endsley, K. A., P. J. Wechsler, T. C. Yokas, A. R. Rodi and W. R. Sand, 1986: University of Wyoming King Air data system. *Proc. of the Second Airborne Science Workshop*. Laramie, Wyoming, Department of Atmospheric Sciences, University of Wyoming, 181–183.
- General Electric Research Laboratory, 1952: History of Project Cirrus, Rep. No. RL-756. Research Publications Services.
- Gordon, G. L., 1986: Cloud Physics Studies in the SPP, Interim Progress Report, 1985–1986. Rep. for Dept. of Atmospheric Sciences, University of Wyoming, 122–135.
- , and J. D. Marwitz, 1986a: APIPs testing using a tracer. Preprints, *10th Conf. on Planned and Inadvertent Weather Modifications*, Arlington, Amer. Meteor. Soc., 61–63.
- , and —, 1986b: Hydrometeor evolution in rainbands over the California valley. *J. Atmos. Sci.*, **43**, 1087–1100.
- , and A. R. Rodi, 1990: Airborne testing for APIPs. Report AS155, Dept. Atmospheric Science, University of Wyoming, Laramie, WY, 122–135.
- Havens, B. S., J. E. Jiusto and B. Vonnegut, 1981: Early history of cloud seeding. *J. Wea. Mod.*, **13**, 14–88.
- Hobbs, P. V., 1985: A case study of scientific amnesia. *Weatherwise*, **38**, 254–258.
- Langmuir, I., V. J. Schaefer, B. Vonnegut, K. Maynard, R. Smith-Johannsen, D. Blanchard and R. E. Falconer, 1948: Final Rep., Project Cirrus, RL140. General Electric Research Laboratory, Requisition 21190 with the Dept. of the Army Project: 3-99-07-022, 119 pp.
- Ludlam, F. H., 1956: Fall-streak holes. *Weather*, **11**, 89–90.
- Mason, B. J., 1957: *The Physics of Clouds*. Clarendon Press, 139.
- Maybank, J., and B. J. Mason, 1959: The production of ice crystals by large adiabatic expansions of water vapour. *Proc. Phys. Soc.*, **74**, 11–16.
- Rangno, A. L., and P. V. Hobbs, 1983: Production of ice particles in clouds due to aircraft penetrations. *J. Climate Appl. Meteor.*, **22**, 214–232.
- , and —, 1984: Further observations of the production of ice particles in clouds by aircraft. *J. Climate Appl. Meteor.*, **23**, 985–987.
- Shaefer, V. J., 1954: Ice crystals formed spontaneously by the rapid expansion of moist air. *J. Colloid Sci.*, **9**, 175–182.
- Scorer, R., and A. Verkaik, 1989: *Spacious Skies*. David and Charles Publishers, 173 pp.
- Vonnegut, B., 1948: Production of ice crystals by the adiabatic expansion of gas. *J. Appl. Phys.*, **19**, 959.
- , 1986: Nucleation of ice crystals in supercooled clouds caused by passage of an airplane. *J. Climate Appl. Meteor.*, **25**, 98.
- Woodley, W. L., and T. J. Henderson, 1990: Atmospheric tests of an organic nucleant in a supercooled fog. *J. Wea. Mod.*, **22**, 127–132.
- , —, B. Vonnegut, G. Gordon, R. Breidenthal and S. Holle, 1990: Results of studies of aircraft produced ice particles (APIPs) in supercooled fog over Mono Lake, California. Final Rep. to National Science Foundation on Grant ATM-8813846, 112 pp.